

# Preparation of Resorcinarene-Functionalized Gold Nanoparticles and Their Catalytic Activities for Reduction of Aromatic Nitro Compounds

Yao, Yong(姚勇) Sun, Yan(孙燕) Han, Ying(韩莹) Yan, Chaoguo\*(颜朝国)

College of Chemistry and Chemical Engineering, Yangzhou University, Yangzhou, Jiangsu 225002, China

Resorcinarene-functionalized gold nanoparticles (AuNPs) were prepared conveniently in aqueous solution in the presence of amphiphilic tetramethoxyresorcinarene tetraaminoamide. The obtained AuNPs were characterized and analyzed by UV-vis, FT-IR, XRD and TEM, respectively. The results showed that the size of AuNPs and the standard deviations were all decreasing with the increase of resorcinarene concentration. In addition, the catalytic activity of the obtained AuNPs in the reduction of aromatic nitro compounds was also investigated. In aqueous solution the reaction follows a first order kinetics and the size of AuNPs has influence on the rate of reduction.

**Keywords** gold nanoparticle, amphiphile, resorcinarene, catalytic reduction, nitrophenol

## Introduction

In recent years, the preparation and application of gold nanoparticles (AuNPs), which have unique optical, electrical, catalytic and other properties,<sup>1,2</sup> constitute a major research area that attracts considerable attention from both fundamental and applied research.<sup>3,4</sup> In particular, AuNPs are widely used for different studies due to their chemical stability and easy preparation. Therefore, the controlled preparation of metallic materials in the nanometer range is attracting increasing research efforts. Several preparation methods of AuNPs including aqueous and nonaqueous processes have been developed.<sup>5,6</sup> For the fabrication of AuNPs, it is well known that the reaction medium, reducing agent and the capping agent are three key factors for the preparation and stabilization of the NPs. Among these factors the stabilizers play an essential role in controlling the formation of nanoparticles as well as their dispersion stability.<sup>7</sup> As the third generation of supramolecular hosts, calixarene and resorcinarene are versatile macrocyclic compounds that present a hydrophobic core sandwiched between two functional rims,<sup>8</sup> which can be easily chemically modified and such modification is of interest for promising application in nanomaterials, molecular reorganization and nano devices. Recently, calixarene is well known as protective agents to stabilize and functionalize AuNPs in the emerging areas of nanoscience and technology.<sup>9</sup> Wei and co-workers<sup>10-12</sup> have demonstrated that resorcinarene and its derivatives are good dispersants for stabilizing AuNPs in nonpolar solvents. Furthermore, calixarene-capped nanoparticles have attracted increasing attention in the field of mo-

lecular reorganization.<sup>13</sup> Sanchez-Cortes *et al.*<sup>14</sup> reported the use of calixarene-functionalized AgNPs for polycyclic aromatic hydrocarbons detection by surface-enhanced Raman scattering. Brust *et al.*<sup>15</sup> introduced a very simple route for the preparation of water-soluble calixarene-functionalized AuNPs and demonstrated that in an aqueous environment the calixarene retains its molecular recognition properties. Li *et al.*<sup>16</sup> reported the calixarene-functionalized NPs employed as highly-sensitive luminescence probes for optical recognition of anthracene and pyrene by changing the cavity size of calixarene. However, the investigation of catalytic properties of the calixarene-encapsulated AuNPs is at very beginning.<sup>17</sup> We also used amphiphilic resorcinarene polyaminoamide as stabilizer to protect gold nanoparticles and as template for the fabrication of gold nanoparticle/microtube hybrid material.<sup>18</sup> Recently the C<sub>4</sub> symmetric tetraalkoxyresorcinarene has emerged as a new members of resorcinarene family and have attracted much attention in versatile application fields.<sup>19</sup> In the present study, we wish to report our preliminary results on the preparation of tetramethoxyresorcinarene encapsulated AuNPs with amphiphilic tetramethoxyresorcinarene tetraaminoamide and their catalytic activity on reduction of some aromatic nitro compounds.

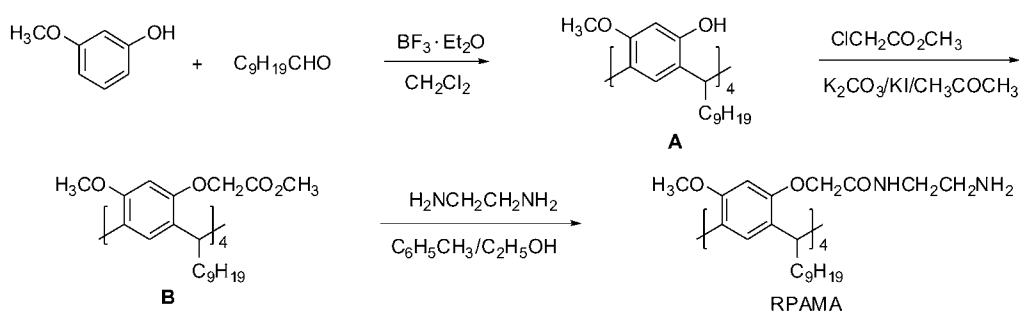
## Results and discussion

The synthetic route for preparing the stabilizer tetramethoxyresorcinarene tetraaminoamide in three steps is shown in Scheme 1. In the first step the tetranonyl tetramethoxyresorcinarene (A) was prepared

\* E-mail: cgyan@yzu.edu.cn

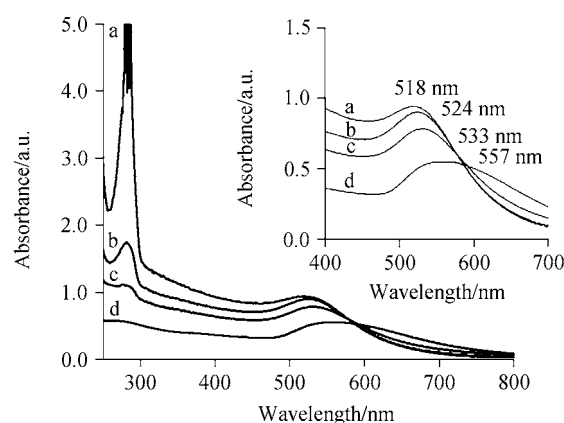
Received September 2, 2009; revised and accepted December 10, 2009.

Project supported by the National Natural Science Foundation of China (Nos. 20672091 and 20972132).

**Scheme 1** Synthetic route of tetramethoxyresorcinarene tetraaminoamide (RPAMA)

by Lewis acid  $\text{BF}_3 \cdot \text{Et}_2\text{O}$  catalyzed condensation of 3-methoxyphenol with decanal according to the published procedure.<sup>19</sup> Then resorcinarene was alkylated with methyl  $\alpha$ -chloroacetate in  $\text{K}_2\text{CO}_3/\text{KI}/\text{acetone}$  system, which is the well established efficient synthetic procedure for the peralkylation of calixarene and resorcinarene.<sup>20,21</sup> The expected tetramethoxyresorcinarene acetate derivative (**B**) was synthesized in 54% yield. In the third step tetramethoxyresorcinarene acetate was ammonolyzed with excess ethylene diamine in refluxing ethanol and toluene to give the desired tetraonyl tetramethoxyresorcinarene tetraaminoamide in 80% yield, which is given the symbol name RPAMA in this text. RPAMA is a new kind of novel amphiphilic molecule with four hydrophilic aminoethylamido groups and four hydrophobic nonyl chains linked to a large resorcinarene cavity.

Gold colloids can be prepared by using tetramethoxyresorcinarene tetraaminoamide (RPAMA) as protective stabilizer according to the same procedure described in our recently published paper.<sup>18</sup> At first an aqueous solution of  $\text{HAuCl}_4$  and RPAMA aqueous solution were mixed. Thus  $\text{Au}^{3+}$  ions were absorbed on the RPAMA where they coordinated with aminoamido groups. Subsequent reduction with sodium borohydride yielded RPAMA encapsulated AuNPs, which are soluble in water and stable for several months. Figure 1 shows the representative UV-vis spectra of gold colloids stabilized with RPAMA at its different concentration. Nearly all of the RPAMA-protected gold nanoparticles displayed the characteristic optical signal of gold colloids, a plasmon resonance in the visible region within the 500–550 nm range.<sup>22</sup> When the concentration of RPAMA was 5, 20, 60 and 200  $\mu\text{mol/L}$ , the maximum absorption wavelengths of gold hydrosols was 557, 533, 524 and 518 nm, respectively. The surface-plasmon absorption band undergoes a blue shift from 557 to 518 nm with the increase of RPAMA concentration. This shift might be due to the decrease in the size of AuNPs formed. Additionally the intensity of AuNPs absorption peak increases with increasing RPAMA concentration. The result suggests that the growth rate of particles is fast and thus larger-sized gold nanoparticles would be obtained at the lower concentration of RPAMA in the system.

**Figure 1** UV-vis spectra of gold colloids stabilized by RPAMA at different concentrations.  $c/(\mu\text{mol} \cdot \text{L}^{-1})$ : (a) 200, (b) 60, (c) 20, (d) 5.

Typical TEM images and histograms of size distribution of RPAMA-capped AuNPs at different concentrations are displayed in Figure 2. The average diameters and standard deviations determined from their histograms at 5, 60 and 200  $\mu\text{mol/L}$  were  $(17.04 \pm 7.95)$ ,  $(9.37 \pm 3.07)$  and  $(6.59 \pm 2.03)$  nm, respectively. As anticipated from the absorption data, polydisperse AuNPs were observed in Figure 2a, which were obtained by using RPAMA as capping agent at lower concentration. With the increasing of stabilizer concentration, spherical AuNPs together with a few triangular AuNPs appear (Figure 2b). In addition, spherical AuNPs with a relatively narrow particle size distribution were also observed, as shown in Figure 2c, which were obtained at the concentration of 200  $\mu\text{mol/L}$ .

The exact capping mechanism of RPAMA on the formation of AuNPs is interesting topics of the current investigation, which has been established in our previous work by using similar amphiphilic octaaminoamido resorcinarene for the preparation of AuNPs.<sup>18a,18b</sup> RPAMA acts as both a template for the preparation of monodisperse AuNPs and a stabilizer. When the appropriate amount of reducing agent sodium borohydride was added into the above solution, the RPAMA-stabilized gold hydrosol was prepared. The timely and effective protection of RPAMA for the separated AuNPs prevents particles from aggregating.

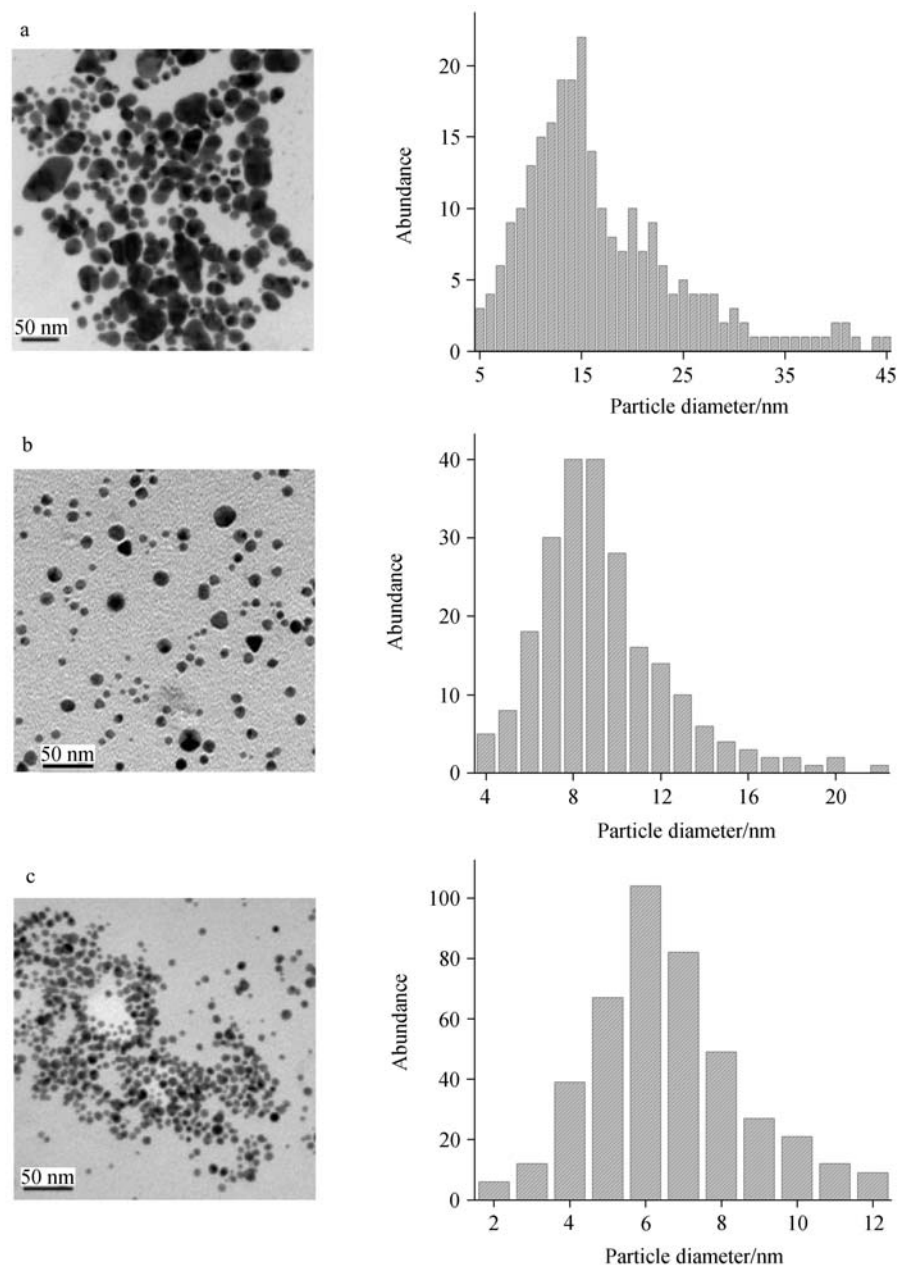


**Figure 2** TEM micrographs of the Au nanoparticles capped by RPAMA at different concentration.  $c/(\mu\text{mol}\cdot\text{L}^{-1})$ : (a) 5, (b) 60, (c) 200.

A comparison of the two FT-IR spectra not only supported the presence of resorcinarene molecules on gold nanoparticles, but also revealed the nature of interaction of resorcinarene molecules with the AuNPs.<sup>23</sup> The features of the pure RPAMA spectrum in the region of  $3000\text{--}2800\text{ cm}^{-1}$  are similar to those of the spectra of the surface-bound RPAMA molecules on AuNPs. It is well known that the symmetric and antisymmetric stretching vibrations of  $\text{CH}_2$  can be used as a sensitive indicator of the ordering of alkyl chains. The shift of vibrations to lower frequency suggests that alkyl chains have more ordered structures. The peak at  $724\text{ cm}^{-1}$  corresponds to the rocking mode of methylene chain for pure RPAMA. When RPAMA coats on the surface of gold nanoparticles, the peak shifts lower to  $721\text{ cm}^{-1}$ . The above results further indicate that RPAMA mole-

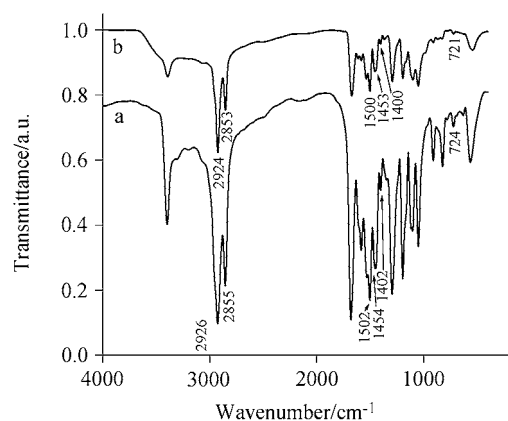


**Figure 3** FT-IR spectra of the pure RPAMA powder (a) and RPAMA-capped gold nanoparticles (b).

cles capping gold nanoparticles have a more ordered structure of the methylene chains.

XRD measurement for RPAMA-capped AuNPs is shown in Figure 4. For the XRD patterns of RPAMA-capped AuNPs, the observed diffraction peaks are those expected for fcc gold on the basis of the bulk lattice constants and are broadened in contrast to the bulk due to the finite size of nanoparticles. The result shows that RPAMA molecules are adsorbed on the surface of gold nanoparticles and play a protecting role for particles.

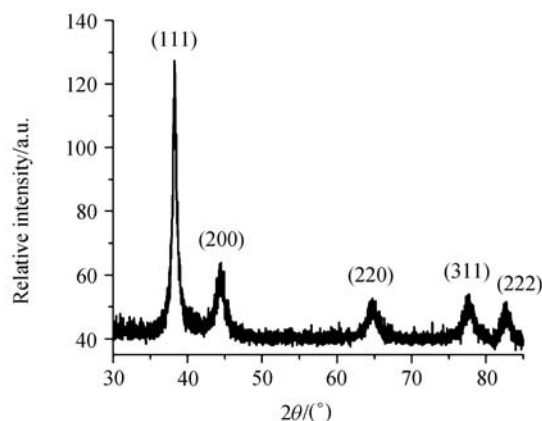


**Figure 4** XRD pattern of RPAMA-capped gold nanoparticles.

In order to test the catalytic activity of the above prepared RPAMA-capped AuNPs, the well established AuNPs catalytic reduction of 4-nitrophenol with  $\text{NaBH}_4$ <sup>24,25</sup> was used as a comparison standard with UV-vis method. It is seen that an absorption peak of 4-nitrophenol undergoes a red shift from 317 to 400 nm (due to the generation of 4-nitrophenolate ion) immediately upon the addition of aqueous solution of  $\text{NaBH}_4$  (500 mmol/L), corresponding to a significant change in solution color from light yellow to yellow-green.

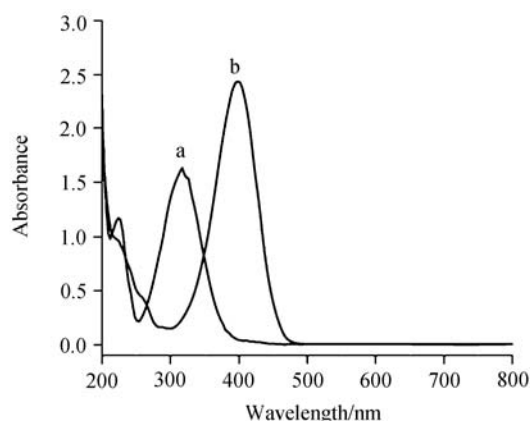


**Figure 5** UV-vis absorption spectra of the 4-nitrophenol before (a) and after (b) the addition of  $\text{NaBH}_4$ .

In the absence of catalyst of AuNPs, the absorption peak at 400 nm remained unaltered for a long duration,

indicating the inability of the strong reducing agent  $\text{NaBH}_4$  itself to reduce 4-nitrophenolate ion.<sup>23</sup> Remarkably, the addition of an aliquot of AuNPs (0.3 mmol/L) dispersion to the mixture caused a fading and ultimate bleaching of the yellow-green color of 4-nitrophenolate ion in aqueous solution, suggesting the occurrence of the reduction reaction. This discoloration was quantitatively monitored by UV-vis spectra with time and has been noted as a successive decrease of the peak height, which was due to the reduction of 4-nitrophenol to 4-aminophenol. Figure 6 verifies this conclusion as well, as the absorption band of 4-nitrophenolate ion at 400 nm decreases and disappears within 13 min after the addition of AuNPs, with the concomitant appearance of two new peaks at 300 and 230 nm, respectively (attributed to the generation of 4-aminophenol).

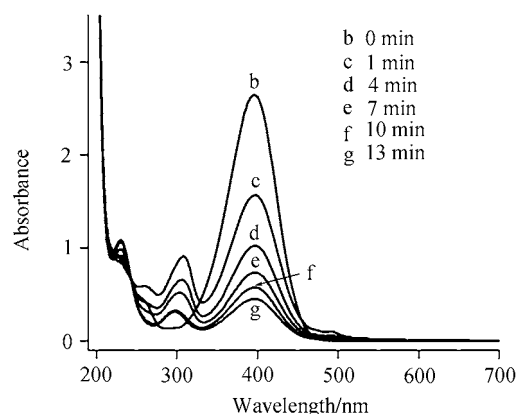


**Figure 6** Successive UV-vis absorption spectra of the reduction of 4-nitrophenol by  $\text{NaBH}_4$  in the presence of RPAMA-capped AuNPs of  $(9.37 \pm 3.07)$  nm as catalyst.

Since the concentration of  $\text{NaBH}_4$  added in the system is much higher in comparison with that of 4-nitrophenol, it is reasonable to assume that the concentration of  $\text{BH}_4^-$  remains constant during the reaction. In this paper, pseudo-first-order kinetics could be used to evaluate the kinetic reaction rate of the current catalytic reaction, together with the UV-vis spectra in Figure 6. As expected, a good linear correlation of  $\ln A$  versus time was obtained, and the kinetic reaction rate constant is estimated to be  $(2.32 \times 10^{-3}) \text{ s}^{-1}$  (Figure 7). This value is comparable to that of other nanoparticle catalysts for the reduction of 4-nitrophenol in the presence of  $\text{NaBH}_4$ . The catalysis of the AuNPs is possibly due to the efficient electron transfer from  $\text{BH}_4^-$  ion to nitro compounds mediated by the higher driving force of particle-mediated electron transfer caused by their large Fermi level shift in the presence of highly electron-injecting species such as borohydride ions.<sup>26</sup>

When the same experiment was conducted with AuNPs of  $(17.04 \pm 7.95)$  nm, the peak due to 4-nitrophenolate ion at 400 nm remains unaltered for a long duration. The kinetic reaction rate constant is esti-

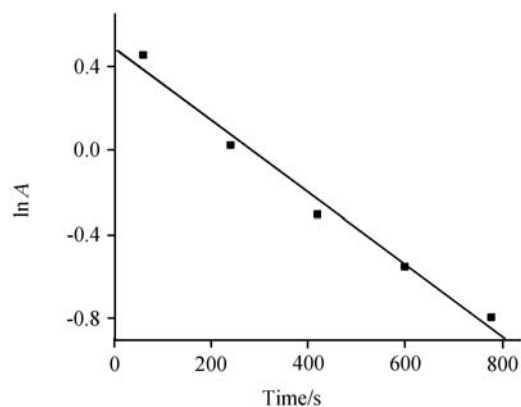


**Figure 7** Plot of  $\ln A$  against time for the Au nanoparticles catalyzed reduction of 4-nitrophenol.

mated to be  $(1.29 \times 10^{-4}) \text{ s}^{-1}$ , indicating the very lower catalytic properties of the larger AuNPs for reduction of 4-nitrophenol. When the same experiment was conducted with AuNPs of  $(6.59 \pm 2.03) \text{ nm}$  (Figure 9) the absorption band of 4-nitrophenolate ion at 400 nm decreases and disappears within 3 min after the addition of AuNPs. Thus the small AuNPs show greater catalytic property for reduction of 4-nitrophenol. Remarkably, the size of the AuNPs showed obvious impact on the reduction rate, the rate for the reduction of 4-nitrophenol decreased with increasing of the size of as-prepared AuNPs.<sup>23</sup> It is interesting to compare the catalytic activities for the reduction of 4-nitrophenol by the size of AuNPs used. The order of the catalytic property is AuNPs  $(6.59 \pm 2.03) \text{ nm} >$  AuNPs  $(9.37 \pm 3.07) \text{ nm} >$  AuNPs  $(17.04 \pm 7.95) \text{ nm}$ . The origin of this order clearly lies in the reaction natures of mechanism. The rate of electron transfer at the metal surface can be influenced by the diffusion of 4-nitrophenol to the metal surfaces and the interfacial electron transfer and diffusion of 4-aminophenol away from the surface.

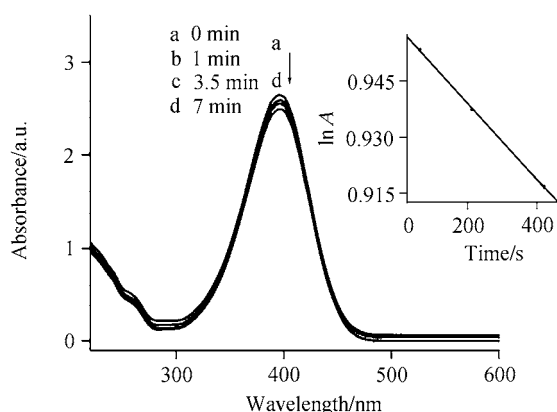


**Figure 8** Successive UV-vis spectra of the reduction of 4-nitrophenol by  $\text{NaBH}_4$  in the presence of RPAMA-capped AuNPs of  $(17.04 \pm 7.95) \text{ nm}$  as catalyst.

The catalytic ability of AuNPs for other aromatic nitro compounds was also investigated under similar reaction conditions with the reduction of 4-nitrophenol.

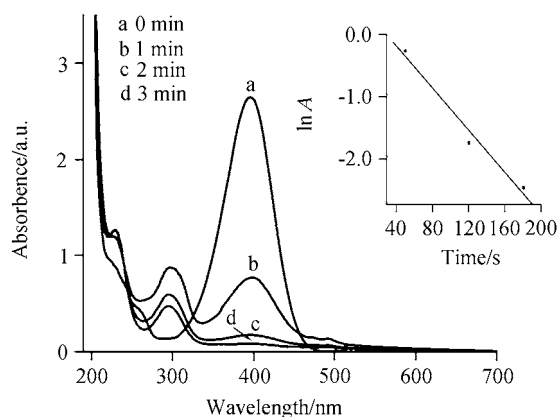


**Figure 9** Successive UV-vis spectra of the reduction of 4-nitrophenol by  $\text{NaBH}_4$  in the presence of RPAMA-capped AuNPs of  $(6.59 \pm 2.03) \text{ nm}$  as catalyst.

3-Nitrophenol and 2-nitrophenol could be reduced with  $\text{NaBH}_4$  with small size of AuNPs as catalyst and their rate of reduction has been studied. As shown in Figure 10a, time dependent reduction of 3-nitrophenol was observed by the successive decrease in the absorbance value at 400 nm. Figure 10b shows the reduction reaction was completed in 25 min, which is relatively longer than 3-nitrophenol and 4-nitrophenol. Thus three isomers of nitrophenol show the relative velocity for cata-

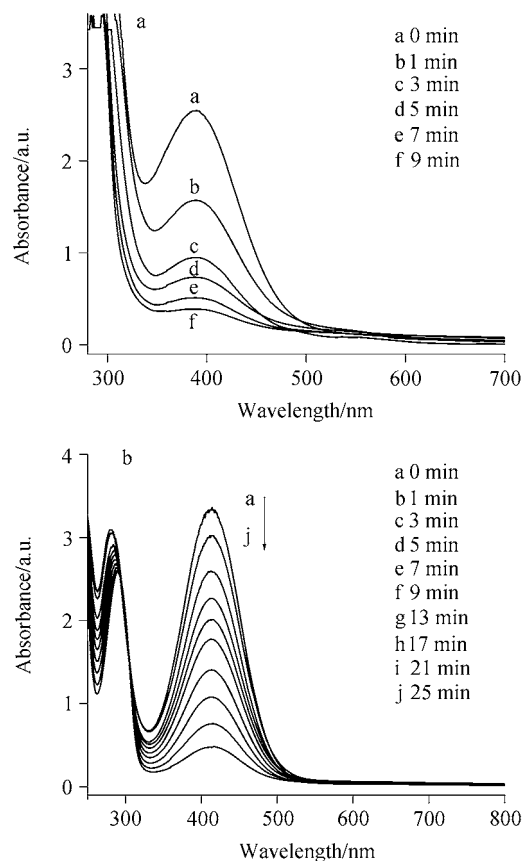


**Figure 10** Successive UV-vis absorption spectra of the reduction of (a) 3-nitrophenol and (b) 2-nitrophenol by  $\text{NaBH}_4$  in the presence of RPAMA-capped AuNPs of  $(6.59 \pm 2.03) \text{ nm}$  as catalyst.

lytic reduction in the series of 4-nitrophenol > 3-nitrophenol > 2-nitrophenol.

Furthermore, the catalyst reduction of 4-nitroaniline was also conducted with the use of AuNPs as catalyst. As shown in Figure 11, the reaction completed within 14 min. This result shows that the RPAMA-capped AuNPs have very potential catalytic ability for reduction of the different kinds of aromatic nitro compounds.

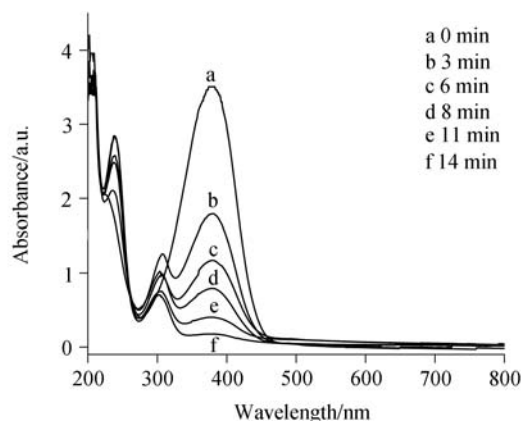


**Figure 11** Successive UV-vis absorption spectra of the reduction of 4-nitroaniline by  $\text{NaBH}_4$  in the presence of RPAMA-capped AuNPs of  $(6.59 \pm 2.03)$  nm as catalyst.

## Experimental

### Materials and characterization

3-Methoxyphenol, methyl chloroacetate, ethylenediamine were purchased from Alfa. Hydrochloroauric acid ( $\text{HAuCl}_4$ ), sodium borohydride ( $\text{NaBH}_4$ ), 2-nitrophenol, 3-nitrophenol, 4-nitrophenol and 4-aminophenol were of reagent grade and were purchased from Shanghai Chemical Reagent Co. Double distilled water was used through-out the experiment.  $\text{NaBH}_4$  solution was prepared in ice-cold distilled water. All the glassware was cleaned by soaking in aqua regia and finally washing with doubly distilled water.

UV-vis spectroscopy of the samples were recorded on a UV-2550 PC UV-vis spectrometer (Shimadzu), the spectral background absorption was subtracted by means of the UV-vis spectrum of water. The morphology and size of the Au hydrosol was investigated on a Philips TECNAI-12 TEM instrument operated at an accelerating voltage of 120 kV. Samples of gold nanoparticles for TEM studies were prepared by placing drops of the solutions onto 200 mesh copper grids covered by Formvar film. Fourier transmission infrared spectra of the samples were collected in the transmission mode on a Nicolet 740 FT-IR spectrometer. The spectra were obtained over 100 scans from which a background spectrum (empty cell) was automatically subtracted. XRD data were obtained with a graphite monochromatic device and Cu  $K\alpha$  radiation ( $\lambda = 0.15406$  nm) on the D8 Advance Super speed Powder Diffractometer (Bruker), operated in the  $\theta : 2\theta$  mode

primarily in the  $20^\circ$ – $85^\circ$  ( $2\theta$ ) range and step-scan of  $2\theta = 0.04^\circ$ . The tube voltage was 80 kV, and the tube current was 200 mA.

### Synthesis of the tetramethoxyresorcinarene tetraaminoamide stabilizer

**2,8,14,20-Tetranonyl-4,10,16,22-tetrahydroxy-6,12,18,24-tetramethoxyresorcinarene<sup>19a</sup>** A solution of 3-methoxyphenol (50 mmol, 6.20 g) and decanal (50 mmol, 7.80 g) in dichloromethane (25 mL) was cooled with ice bath. The boron trifluoride etherate (100 mmol, 14.20 g) was added dropwise to the solution and the mixture was stirred at room temperature for 24 h. The reaction mixture was then washed with water ( $50 \text{ mL} \times 2$ ), dried over  $\text{MgSO}_4$  and the solvent removed under reduced pressure to give a dark red oil. After adding 10 mL of methanol and stirred for some time, the white solid **A** was obtained in 84% yield. m.p.  $98$ – $100^\circ \text{C}$ ;  $^1\text{H}$  NMR ( $\text{CDCl}_3$ , 300 MHz)  $\delta$ : 7.53 (s, 4H, OH), 7.21 (s, 4H, ArH), 6.34 (s, 4H, ArH), 4.26–4.25 (m, 4H, CHAr), 3.82 (s, 12H,  $\text{OCH}_3$ ), 2.17 (s, 8H,  $\text{CH}_2$ ), 1.31–1.29 (m, 56H,  $\text{CH}_2$ ), 0.88 (t,  $J = 7.2$  Hz, 12H,  $\text{CH}_3$ ); IR (KBr)  $\nu$ : 3387, 2924, 2852, 1619, 1588, 1498, 1462, 1298, 1235, 1194, 1162, 1093, 899, 837, 723  $\text{cm}^{-1}$ .

**2,8,14,20-Tetranonyl-4,10,16,22-tetra(methoxycarbonylmethoxyl)-6,12,18,24-tetramethoxyresorcinarene<sup>19b</sup>** A mixture of **A** (5.0 mmol, 4.76 g), anhydrous potassium carbonate (70 mmol, 10.6 g) and potassium iodide (8.0 mmol, 1.3 g) in dry acetone (150 mL) was heated to refluxing for at least 0.5 h. Then methyl chloroacetate (50 mmol, 5.45 g) was added and the reaction mixture was refluxed for 7 d. Then the potassium carbonate was removed by filtration. After evaporation of the solvent and excessive methyl chloroacetate the red oil residue was titrated with 10 mL of ethanol to give white crystal **B** in 54% yield. m.p.  $80$ – $81^\circ \text{C}$ ;  $^1\text{H}$  NMR ( $\text{CDCl}_3$ , 300 MHz)  $\delta$ : 6.61 (s, 4H, ArH), 6.29 (s, 4H, ArH), 4.50 (t,  $J = 7.2$  Hz, 4H, CHAr), 4.20 (d,  $J = 15.6$  Hz, 4H,  $\text{OCH}_2$ ), 4.01 (d,  $J = 16.2$  Hz, 4H,  $\text{OCH}_2$ ), 3.77 (s, 12H,  $\text{OCH}_3$ ), 3.62 (s, 12H,  $\text{OCH}_3$ ), 1.81–1.23 (m, 64H,  $\text{CH}_2$ ), 0.85 (t,  $J = 7.2$  Hz, 12H,  $\text{CH}_3$ ); IR (KBr)  $\nu$ : 2922, 2852, 1773, 1752, 1612, 1502, 1436, 1405, 1375, 1304, 1193, 1126, 1076, 911, 812, 721  $\text{cm}^{-1}$ .

**2,8,14,20-Tetranonyl-4,10,16,22-tetraaminoethyl-carbamoylmethoxyl-6,12,18,24-tetramethoxyresorcinarene** A mixture of **B** (1.0 mmol, 1.00 g) and 1,2-diaminoethane (8.0 mL) in ethanol (15 mL) and toluene (15 mL) was reflux for 24 h. The organic solvent and excessive amine were removed under vacuum. The residue was crystallized in ethanol to give white solid **C** with RPAMA as its symbol in this text. Yield 80%; m.p.  $128$ – $130^\circ \text{C}$ ;  $^1\text{H}$  NMR ( $\text{CDCl}_3$ , 300 MHz)  $\delta$ : 7.04 (s, 4H, ArH), 6.71 (s, 4H, ArH), 4.51–4.48 (m, 4H,  $\text{OCH}_2$ ), 4.40–4.38 (m, 4H,  $\text{OCH}_2$ ), 4.26–4.24 (m, 4H, CHAr), 3.67 (s, 12H,  $\text{OCH}_3$ ), 3.40–3.27 (m, 8H,  $\text{NCH}_2$ ), 2.81–2.80 (m, 8H,  $\text{NCH}_2$ ), 1.29–1.23 (m, 64H,  $\text{CH}_2$ ), 0.86 (t,  $J = 7.2$  Hz, 12H,  $\text{CH}_3$ ); IR (KBr)  $\nu$ : 3396, 2925, 2853, 1678, 1584, 1502, 1444, 1403, 1297,

1196, 1126, 1050, 911, 821  $\text{cm}^{-1}$ .

### Preparation of gold nanoparticles capped with RPAMA

RPAMA-coated gold nanoparticles were prepared by the reduction of  $\text{HAuCl}_4$  solution as described in our previous reports.<sup>18</sup> In a typical experiment, an aqueous solution of  $\text{HAuCl}_4$  (0.20 mL, 9.7 mmol/L) and RPAMA aqueous solution (6.0 mL) were mixed in a 100 mL round flask. Then, sodium borohydride aqueous solution (0.40 mL, 0.1 mol/L) was injected into the above solution under vigorous stirring, and the resorcinarene-capped AuNPs were immediately obtained.

### Procedures for the reduction of nitro compounds using RPAMA-coated AuNPs

The catalytic reduction of 4-nitrophenol was studied as follows. In the standard quartz cuvette with 1-cm path length, 6 mL of 0.15 mmol/L 4-nitrophenol and 1 mL of 0.5 mol/L  $\text{NaBH}_4$  aqueous solution was added. Then the addition of 0.1 mL of Au colloid to the mixture caused the decrease in the intensity of the peak of 4-nitrophenol. The absorption spectra were recorded every 3 min in the range of 200–700 nm at room temperature. The control experiment was also carried out using the mixtures of  $\text{NaBH}_4$  and 4-nitrophenol. The absorption spectrum of 4-nitrophenol was unaltered. The same procedure was applied to the catalytic reduction of 2-nitrophenol, 3-nitrophenol and 4-nitroaniline.

### Conclusion

We have successfully synthesized a novel amphiphilic resorcinarene surfactant (RPAMA) with four amine groups that can become both template and stabilizer for gold nanoparticles. It is found that the particle size of AuNPs prepared using RPAMA decreases with an increase in the molar ratio of  $[\text{RPAMA}]/[\text{Au}^{3+}]$ , and their standard deviation also becomes small. Stable AuNPs are obtained by the RPAMA adsorbing on the gold surfaces as a bilayer. The combination of catalytic qualities of AuNPs with  $\text{NaBH}_4$  reduces aromatic nitro compounds to amines in aqueous media. A distinct difference in the catalytic activity is observed with the change of the AuNPs size. This suggests that the rate constant is significantly affected by the size of the RPAMA adsorbing on the nanoparticles. The rate of reduction has been observed to follow the sequence: 4-nitrophenol > 3-nitrophenol > 2-nitrophenol.

### References

- (a) Corain, B.; Schmid, G.; Toshima, N. *Metal Nanoclusters in Catalysis and Materials Science: The Issue of Size Control*, Elsevier, Amsterdam, **2008**.  
(b) Daniel, M. C.; Astruc, D. *Chem. Rev.* **2004**, *104*, 293.
- (a) Cui, Y.; Wei, Q.; Park, H.; Lieber, C. M. *Science* **2001**, *293*, 1289.  
(b) Katz, E.; Willner, I. *J. Am. Chem. Soc.* **2002**, *124*, 10290.
- (a) Ung, T.; Liz-Marzan, L. M.; Mulvaney, P. *J. Phys. Chem. B* **2001**, *105*, 3441.  
(b) Poznyak, S. K.; Talapin, D. V.; Shevchenko, E. V.; Weller, H. *Nano Lett.* **2004**, *4*, 693.  
(c) Zhao, M.; Crooks, R. M. *Adv. Mater.* **1999**, *11*, 217.
- (a) Rosi, N. L.; Giljohann, D. A.; Thaxton, C. S.; Lytton-Jean, A. K. R.; Han, M. S.; Mirkin, C. A. *Science* **2006**, *312*, 1027.
- Bowman, M. C.; Ballard, T. E.; Ackerson, J. C.; Feldheim, D. L.; Margolis, D. M.; Melander, C. *J. Am. Chem. Soc.* **2008**, *130*, 6896.
- (a) Collier, C. P.; Saykally, R. J.; Shiang, J. J.; Henrichs, S. E.; Heath, J. R. *Science* **1997**, *277*, 5334.  
(b) McMahon, J. M.; Emory, S. R. *Langmuir* **2007**, *23*, 1414.
- Liu, Y.; Male, K. B.; Bouverette, P.; Luong, J. H. T. *Chem. Mater.* **2003**, *15*, 4172.
- (a) Rebek, J. Jr. *Chem. Commun.* **2007**, 2763.  
(b) Biro, S. M.; Rebek, J. Jr. *Chem. Soc. Rev.* **2007**, *36*, 93.
- Wei, A. *Chem. Commun.* **2006**, 1581.
- (a) Stavens, K. B.; Pusztay, S. V.; Zou, S.; Andres, R. P.; Wei, A. *Langmuir* **1999**, *15*, 8337.  
(b) Balasubramanian, R.; Kim, B.; Tripp, S. L.; Wang, X.; Lieberman, M.; Wei, A. *Langmuir* **2002**, *18*, 3676.  
(c) Kim, M. B.; Carignano, A.; Tripp, S. L.; Wei, A. *Langmuir* **2004**, *20*, 9360.
- (a) Kim, B.; Tripp, S. L.; Wei, A. *J. Am. Chem. Soc.* **2001**, *123*, 7955.  
(b) Zhao, Y.; Pérez-Segarra, W.; Shi, Q. C.; Wei, A. *J. Am. Chem. Soc.* **2005**, *127*, 7328.
- (a) Balasubramanian, R.; Xu, J.; Kim, B.; Sadtler, B.; Wei, A. *J. Dispers. Sci. Technol.* **2001**, *22*, 485.  
(b) Wei, A.; Kim, B.; Pusztay, S. V.; Tripp, S. L.; Balasubramanian, R. *J. Inclusion Phenom. Macrocycl. Chem.* **2001**, *41*, 83.
- (a) Pusztay, S. V.; Wei, A.; Stavens, K. B.; Andres, R. P. *Supramol. Chem.* **2002**, *14*, 291.  
(b) Kim, B.; Balasubramanian, R.; Perez-Segarra, W.; Wei, A.; Decker, B.; Mattay, J. *Supramol. Chem.* **2005**, *17*, 173.
- Guerrini, L.; Garcia-Ramos, J. V.; Domingo, C.; Sanchez-Cortes, S. *Langmuir* **2006**, *22*, 10924.
- Tshikhudo, T. R.; Demuru, D.; Wang, Z.; Brust, M.; Secchi, A.; Arduini, A.; Pochini, A. *Angew. Chem., Int. Ed.* **2005**, *44*, 2913.
- (a) Li, H.; Qu, F. *Chem. Mater.* **2007**, *19*, 4148.  
(b) Li, H.; Qu, F. *J. Mater. Chem.* **2007**, *17*, 3536.
- (a) Cui, H.; Guo, J. Z.; Li, N.; Liu, L. J. *J. Phys. Chem. C* **2008**, *112*, 11319.  
(b) Esumi, K.; Isono, R.; Yoshimura, T. *Langmuir* **2004**, *20*, 237.  
(c) Hayakawa, K.; Yoshimura, T.; Esumi, K. *Langmuir* **2003**, *19*, 5517.
- (a) Shen, M.; Sun, Y.; Han, Y.; Yao, Y.; Yan, C. G. *Langmuir* **2008**, *24*, 13161.  
(b) Shen, M.; Chen, W. F.; Sun, Y.; Yan, C. G. *J. Phys. Chem. Sol.* **2007**, *68*, 2252.  
(c) Sun, Y.; Yan, C. G.; Yao, Y.; Han, Y.; Shen, M. *Adv.*

- Funct. Mater.* **2008**, *18*, 3981.
- 19 (a) McIldowie, M. J.; Mocerino, M.; Skelton, B. W.; White, A. H. *Org. Lett.* **2000**, *2*, 3869.  
(b) Kales, M.; Avena, C.; Kohler, M.; Inoue, M.; Wada, T.; Inue, Y.; Mattay, J. *Eur. J. Org. Chem.* **2003**, 1404.  
(c) Buckley, B. R.; Boxhall, J. Y.; Page, P. C. B.; Chan, Y.; Elsegood, M. R. J.; Heaney, H.; Holmes, K. E.; McIldowie, M. J.; McKee, V.; McGrath, M. J.; Mocerino, M.; Poulton, A. M.; Sampler, E. P.; Skelton, B. W.; White, A. H. *Eur. J. Org. Chem.* **2006**, 5117.
- 20 Li, L.; Gu, W. W.; Yan, C. G. *Chin. J. Chem.* **2009**, *27*, 1975.
- 21 Chen, J.; Chen, W. F.; Yan, C. G. *Chin. J. Chem.* **2009**, *27*, 1697.
- 22 Link, S.; El-Sayed, M. A. *J. Phys. Chem. B* **1999**, *103*, 4212.
- 23 Sau, T. K.; Murphy, C. J. *Langmuir* **2005**, *21*, 2923.
- 24 (a) Kumar, S. S.; Kumar, C. S.; Mathiyarasu, J.; Phani, K. L. *Langmuir* **2007**, *23*, 3401.  
(b) Pradhan, N.; Pal, A.; Pal, T. *Langmuir* **2001**, *17*, 1800.  
(c) Hayakawa, K.; Yoshimura, T.; Esumi, K. *Langmuir* **2003**, *19*, 5517.  
(d) Esumi, K.; Isono, R.; Yoshimura, T. *Langmuir* **2004**, *20*, 237.
- 25 (a) Liu, J. C.; Qin, G. W.; Raveendran, P.; Ikushima, Y. *Chem. Eur. J.* **2006**, *12*, 2131.  
(b) Esumi, K.; Miyamoto, K.; Yoshimura, T. *J. Colloid Interface Sci.* **2002**, *254*, 402.  
(c) Pradhan, N.; Pal, A.; Pal, T. *Colloids Surf. A* **2002**, *196*, 247.
- 26 (a) Mora-Sero, I.; Bisquert, J. *Nano Lett.* **2003**, *3*, 945.  
(b) Jakob, M.; Levanon, H.; Kamat, P. V. *Nano Lett.* **2003**, *3*, 353.

(E0909021 Pan, B.; Lu, Z.)